RESEARCH ARTICLE

Editorial Process: Submission:01/05/2022 Acceptance:09/18/2022

Invasion and Metastasis Suppression by Anti-Neonatal Nav1.5 Antibodies in Breast Cancer

Nur Aishah Sharudin[1], Ahmad Hafiz Murtadha Noor Din[1], Irfan Irsyad Azahar[1], Mawaddah Mohd Azlan[1], Nik Soriani Yaacob[2], Maria Elena Sarmiento[3], Armando Acosta Dominguez[3], Noor Fatmawati Mokhtar[1]*

Abstract

Background: Detectable neonatal Nav1.5 (nNav1.5) expression in tumour breast tissue positive for lymph node metastasis and triple-negative subtype serves as a valid tumour-associated antigen to target and prevent breast cancer invasion and metastasis. Therapeutic antibodies against tumour antigens have become the predominant class of new drugs in cancer therapy because of their fewer adverse effects and high specificity. **Objective:** This study was designed to investigate the therapeutic and anti-metastatic potential of the two newly obtained anti-nNav1.5 antibodies, polyclonal anti-nNav1.5 (pAb-nNav1.5) and monoclonal anti-nNav1.5 (mAb-nNav1.5), on breast cancer invasion and metastasis. **Methods:** MDA-MB-231 and 4T1 cells were used as in vitro models to study the effect of pAb-nNav1.5 (59.2 µg/ml) and mAb-nNav1.5 (10 µg/ml) (24 hours treatment) on cell invasion. 4T1-induced mammary tumours in BALB/c female mice were used as an in vivo model to study the effect of a single dose of intravenous pAb-nNav1.5 (1 mg/ml) and mAb-nNav1.5 (1 mg/ml) on the occurrence of metastasis. Real-time PCR and immunofluorescence staining were conducted to assess the effect of antibody treatment on nNav1.5 mRNA and protein expression, respectively. The animals' body weight, organs, lesions, and tumour mass were also measured and compared. **Results:** pAb-nNav1.5 and mAb-nNav1.5 treatments effectively suppressed the invasion of MDA-MB-231 and 4T1 cells in the 3D spheroid invasion assay. Both antibodies significantly reduced nNav1.5 gene and protein expression in these cell lines. Treatment with pAb-nNav1.5 and mAb-nNav1.5 successfully reduced mammary tumour tissue size and mass and prevented lesions in vital organs of the mammary tumour animal model whilst maintaining the animal's healthy weight. mRNA expression of nNav1.5 in mammary tumour tissues was only reduced by mAb-nNav1.5. Conclusion: Overall, this work verifies the uniqueness of targeting nNav1.5 in breast cancer invasion and metastasis prevention, but more importantly, humanised versions of mAb-nNav1.5 may be valuable passive immunotherapeutic agents to target nNav1.5 in breast cancer.

Keywords: Voltage-gated sodium channel- nNav1.5- monoclonal antibody- polyclonal antibody- breast cancer

Asian Pac J Cancer Prev, **23 (9)**, 2953-2964

Introduction

Advanced or metastatic breast cancer management suffers significant drawbacks due to ineffective current breast cancer treatments that focus mainly on primary breast cancer (Bennett et al., 2004; Wang et al., 2017). Consequently, advanced-stage breast cancer patients have the poorest survival rates, contributing to 90% of cancer mortality (Russo, 2016). Understanding cancer's hallmarks, particularly the activation of invasion and metastasis, will aid in discovering molecular therapeutics that prevent cancer growth and spread (Hanahan and Weinberg, 2011).

Ion channels, including voltage-gated sodium channels (VGSCs), are found in various cancers such as breast (Fraser et al., 2005), prostate (Bennett et al., 2004), colon (House et al., 2010), lung (Roger et al., 2007), and gastric (Xia et al., 2016). VGSCs are strongly upregulated in cancer cells and implicated in cell invasion and metastasis through its invadopodia, the leading edge of metastatic cancer cells (Brisson et al., 2011). Classically, this transmembrane protein comprising α and β subunits is known for its roles and functions in generating and propagating action potentials in excitable cells, i.e., neuron and muscle fibers (Diss et al., 2004).

A cardiac isoform of α subunit VGSCs, Nav1.5 encoded by SCN5A gene contributes > 80% of VGSCs expression in aggressive breast cancer cell lines/tissue

*[1]Institute for Research in Molecular Medicine (INFORMM), Universiti Sains Malaysia, Health Campus, 16150 Kubang Kerian, Kelantan, Malaysia. [2]Department of Chemical Pathology, School of Medical Sciences, Universiti Sains Malaysia, Health Campus, 16150 Kubang Kerian, Kelantan, Malaysia. [3]School of Health Sciences, Universiti Sains Malaysia, Health Campus, 16150 Kubang Kerian, Kelantan, Malaysia. *For Correspondence: fatmawati@usm.my*

biopsies as demonstrated by real-time PCR and immuno-cyto/histochemistry (Chioni et al., 2005; Fraser et al., 2005; Brackenbury et al., 2007). Further sequence analysis indicated that the predominant version is the 'neonatal' splice variant, termed as neonatal Nav1.5, nNav1.5 (Chioni et al., 2005). In humans, mice, and rats, the existence of nNav1.5 has been confirmed, and it contains a disrupted D1:S3 with 31 nucleotides different (equal to 7 amino acid changes) from the adult exon (Chioni et al., 2005). In patients, both mRNA and protein expression of nNav1.5 in vitro and tissue biopsies are higher in breast cancer tissues compared to normal breast tissues (Fraser et al., 2005; Yamaci et al., 2017). Importantly, nNav1.5 expression in breast cancer tissues is linked to lymph node metastasis, recurrence, and poor cancer survival (Fraser et al., 2005).

The function of nNav1.5/Nav1.5 in breast cancer aggressiveness and metastasis was first demonstrated using specific VGSCs blockers, tetrodotoxin (TTX), and later, various additional VGSCs small molecule modulator drugs such as channel blocker, ranolazine (Driffort et al., 2014) and phenytoin (Nelson, Yang, Dowle et al., 2015) and channel 'opener', aconitine and anemone toxin (ATX II) (Fraser et al., 2003). These agents, especially those of channel blocker, not only blocked nNav1.5/Nav1.5 channel activity but also suppressed its expression and significantly inhibited various types of cellular behaviours such as directional motility and invasion in vitro (Brackenbury et al., 2007), as well as the ability to metastasize in animal models, in vivo (Driffort et al., 2014; Nelson, Yang, Millican-Slater et al., 2015). Other methods to prove the vital role of nNav1.5/Nav1.5 in breast cancer invasion has also involved the use of siRNA/shRNA (Brackenbury et al., 2007; Nelson ,Yang, Millican-Slateret al., 2015).

Clearly, the uniqueness of nNav1.5 exemplifies its potential as a novel tumour-associated marker for combating aggressive breast cancer. Efforts are already ongoing to re-purpose VGSCs inhibitor drugs for breast cancer treatment (Onkal and Djamgoz, 2009). With antibody-based drugs are now a leading class of biologics for the treatment of cancer (Lu et al., 2020), there also works of antibody with VGSCs blocking ability similar to TTX that suppress breast cancer aggressiveness, a rabbit polyclonal antibody, NESOpAb (Chioni et al., 2005). NESOpAb has not only able to demonstrate its value as 'tool' to detect nNav1.5 but also as therapeutic agent to suppress metastatic cascade of breast cancer (Brackenbury et al., 2007). However, reports of this non-commercialised NESOpAb on breast cancer confined only in vitro and never been tested in vivo. Our group recently obtained two new anti-nNav1.5 mouse polyclonal (pAb-nNav1.5) and monoclonal (mAb-nNav1.5) antibodies and this study was designed to determine the efficacy of targeting nNav1.5 with these antibodies on breast cancer invasion in breast cancer 3D-spheroid culture and animal model of mammary tumours (orthotopic syngeneic mice inoculated with 4T1 cells known to express high nNav1.5 expression).

Materials and Methods

Cell Culture

Human breast cancer cell lines, MDA-MB-231, MCF-7 cells, and mouse mammary cancer cells, 4T1, were attained from the American Type Culture Collection (ATCC, USA). Cells were cultured in Dulbecco's modified Eagle's medium (DMEM) supplemented with fetal bovine serum (5%) and L-glutamine (4 mM) (Nacalai Tesque, Japan) at a constant temperature of 37°C in 5% CO2 and relative humidified atmosphere. Cells were passaged when the confluency reached 80%.

Antibodies and TTX

The peptide sequence of the nNav1.5 specific epitope (15 amino acids in length -VSENIKLGNLSALRC) was obtained from the National Center for Biotechnology Information (NCBI), GenBank: CAC84535.1 (Chioni et al., 2005). The pAb-nNav1.5 antibody was prepared by immunisation of the nNav1.5 peptide into female C57BL/6 mice, and the mAb-nNav1.5 antibody was synthesised from a selected hybridoma clone, both of which were contract produced by Genscript, USA. The purified antibodies were received in lyophilised form and diluted in 1 X Phosphate-buffered saline (PBS) (Nacalai Tesque, Japan). Working concentrations were then diluted in a culture medium to 10 µg/ml and 59.2 µg/ml, respectively, for in vitro studies. Meanwhile, 1 mg/ml of both pAb-nNav1.5 and mAb-nNav1.5 antibodies was used in the animal study. TTX (Tocris Bioscience, UK) was initially prepared with citrate buffer and diluted with molecular grade RNase free water (1st Base, Singapore) to a working concentration of 20 µM.

Real-time reverse transcription-polymerase chain reaction analysis

Total RNA was extracted using the Sepasol method according to the protocol provided by the manufacturer (Nacalai Tesque, Japan). One µg of total RNA was converted to cDNA using ReverTra Ace® qPCR RT Master Mix with gDNA Remover (Toyobo, Japan). Real-time PCR was performed using SensiFAST SYBR Hi-ROX kit (Bioline, UK) in triplicates. Sequence primers used were as follows:

B-actin forward:
5'- ATTGCCGACAGGATGCAGAAG-3'
B-actin reverse:
5'- TAGAAGCATTTGCGGTGGACG-3'
GAPDH forward:
5'- TGACTTCAACAGCGA-3'
GAPDH reverse:
5'- GGGTCTTACTCCTTGGAGGC-3'
nNav1.5 mouse forward:
5'- TGGCGTATGTATCAGAGAATATAAAGC-3'
nNav1.5 mouse reverse"
5'- CTGGAATAACTGAAATCGTTTTCAGAGC-3'
nNav1.5 human forward:
5'- CTGCACGCGTTCACTTTCCT-3'
nNav1.5 human reverse: 5'-
GACAAATTGCCTAGTTTTATATTT-3'

Real-time PCR was performed on ABI Prism 7000

Sequence Detection System (Life Technologies, USA). The amplification condition was set in Table 1:

Table 1. Cycling Condition for RT-PCR

	Cycle	Temperature (°C)	Duration
Initial activation	1	95	5 minutes
	35	95	10 seconds
		60	30 seconds
Dissociation	1	95	15 seconds
		60	20 seconds
		95	15 seconds

Ct values of target genes were normalised to β-actin (for human cell lines) and GAPDH (for mouse cell lines), and the relative mRNA expression of target genes was calculated using the $2^{-\Delta Ct}$ method (Livak and Schmittgen, 2001).

Immunostaining and microscopic imaging

Cells (3 X 10^4 cells/500 µl) were cultured overnight on round coverslips (13 mm diameter) that were initially coated with 0.1 mg/ml of Poly-l-lysine (500 µl/well) before the cell seeding. Then, treatment media [mAb-nNav1.5 (1:100), pAb-nNav1.5 (1:10) antibodies, TTX (10 µM)] were added and incubated for 24h at 37°C, 5% CO_2. Cells were washed with 1 X PBS and fixed with ice-cold acetone for 1 min. Then, the cells were incubated with Concanavalin A FITC-conjugated (Sigma) at 1:100 dilution for 45 min, left in humidified and dark incubation chamber on a rocker at room temperature. Blocking with 2% bovine serum albumin (BSA) was conducted for 30 min to reduce the background during the imaging process. nNav1.5 was detected using a primary antibody (diluted in antibody signal enhancer (ASE) (Rosas-Arellano et al., 2016) for one hour in humidified chamber followed by another one-hour incubation with secondary anti-mouse antibody-conjugated AlexaFluor-555 (Santa Cruz Biotechnology, USA) (diluted in permeabilisation buffer). Finally, the coverslips were mounted using a mounting medium with DAPI (Nacalai Tesque, Japan). The fluorescence image of each coverslip was captured using Leica Inverted DMi8 Fluorescence and DFC 365 FX camera (Germany). FITC, AlexaFluor-555, and DAPI were excited with 488, 555, and 461 nm laser lines, respectively. The images were captured under 40 X magnification, where an average of six single scans were taken. Image analysis was performed using Leica Application Suites X (LAS X) software (Germany).

Invasion assay on 3D-spheroid

Spheroids of MDA-MB-231 and 4T1 cells were generated according to Cultrex 96-Well 3D Spheroid Basement Membrane (BME) Cell Invasion kit (Merck, Germany). 2 X 10^3 cells/50 µl were seeded in each well of upper low attachment (ULA) 96-well plate. 1 X spheroid formation ECM, which consisted of extracellular matrix proteins obtained from murine EHS sarcoma cells and collagen as a medium, aided spheroid formation. A swing bucket rotor centrifuge was employed to aid in the formation of spheroids, followed by 72 hours of incubation at 37°C with 5% CO2. Then, the spheroids were loaded with an invasion matrix and incubated for one hour at 37°C. A warm fresh complete DMEM (100 µl) was added and incubated at 37oC for 7 days with the treatment agents, pAb-nNav1.5 (3:7 = 177 µg/ml, mAb-nNav1.5 antibodies (1:9 = 108.8 µg/ml), and TTX (10 µM). Daily spheroid images were captured with a Leica Inverted DMi8 Fluorescence microscope and a DFC 365 FX camera at 10 X magnification (Germany).

The images were then analysed with Image J software, and the invasion area was determined using the spheroids' perimeter diameters. The invasion area was then normalised using the Day 0 reading before the invasion assay. A double relative calculation was used to compare spheroid invasion to untreated spheroids using 2-way ANOVA statistical analysis. The double relative calculation used in the 3D-spheroid invasion assay was as follows:

$$Normalized\ reading = \frac{Perimeter\ diameter\ of\ treated\ spheroid}{Perimeter\ diameter\ of\ D0\ spheroid} \times 100$$

$$Percentage\ of\ invasion\ reduction = \frac{Normalized\ treated\ spheroid}{Normalized\ untreated\ \ spheroid} \times 100$$

Syngeneic mouse model of an orthotopic-induced mammary tumour

The use of animals in this study was evaluated and approved by the Universiti Sains Malaysia Animal Ethics Committee USM/IACUC/2018/(113)(934). Eighteen female BALB/c mice at 11-12 weeks of age from Animal Research and Service Centre (ARASC), USM Health Campus, were kept in polypropylene cages with stainless steel wire top clips. The ambient temperature was kept around 22 ± 3 °C, the humidity was maintained between 50 and 60%, and the light and dark cycle was kept consistent for 12 hours (light 0700-1900). All mice were fed conventional mice pellets, with each mouse receiving 10 g pellets daily. There was also an unlimited supply of tap water ad libitum given. The cages and dust-free softwood chip bedding (Chipsi, Germany) were changed weekly or as needed. Before the investigation, all mice were given a seven-day acclimatisation period.

The mice were divided into three groups 1) PBS-treated, 2) mAb-nNav1.5 treated, and 3) pAb-nNav1.5 treated. The study lasted 49 days, beginning at the time of 4T1 tumour induction (after one week of acclimatisation) and ending when the animals were euthanised (7 weeks of experiment or before animals were moribund). Under light anaesthesia, the fur over the lateral thorax was shaved, and 0.1 ml (1 x 10^5 cells) of 4T1 tumour cells was subcutaneously injected into the mammary fat pads by gently penetrating the skin of the mice. The onset of the primary tumour was monitored daily by palpating the injection area with the index finger and thumb for its presence, that usually developed within one week. Tumour volume was measured twice a week using a Vernier calliper and calculated using the following formula:

$$\text{Tumour volume} = \frac{ab^2}{2}$$

(a = length of tumor, b = width of tumor) (Faustino-

Rocha et al., 2013).

For each group of animals, weight and signs of discomfort or pain were recorded. After three weeks of tumor inoculation (day 21), one dose treatment of PBS (200 µl), pAb-nNav1.5 (1 mg/ml = 200 µl), and mAb-nNav1.5 (1 mg/ml = 200 µl) was intravenously injected into the animals. The observation was carried out for four weeks to monitor the effects of the treatment agents.

The mice were sacrificed when the tumour reached 14 to 16 mm (approximately seven weeks post-injection) or when the mice became moribund. Animals were anaesthetised with sodium pentobarbital (Vetoquinol, UK), and organs comprising the lung, liver, intestines, and spleen were extracted and stored at -20oC until further use. The size and weight of the extracted organs and tumours were determined. The extracted organs were also observed for the presence of any macro-metastasis.

Statistical analysis

Data are presented as mean and standard error mean (SEM) unless stated otherwise. GraphPad Version 7.0 was used for statistical analysis. T-tests were used to examine the statistical significance of pairs. Unless otherwise specified, multiple comparisons were performed using ANOVA. At $p < 0.05$, the results were considered significant.

Results

Basal expression of nNav1.5 in breast cancer cells

Real-time PCR was used to assess and compare the mRNA expression level of nNav1.5 (nSCN5A) in aggressive human breast cancer cell lines; MDA-MB-231 and mouse mammary cancer cell lines, 4T1 in comparison to MCF-7 cells (weakly invasive human breast cancer cells). 4T1 cells in this study served as the link between the in vivo studies in mice and the in vitro studies in human cell lines. The expression of nSCN5A in MDA-MB-231 and 4T1 cells (highly invasive cancer cells) were significantly higher than in MCF-7 cells, $p < 0.05$ and $p < 0.001$ (Figure 1).

mAb-nNav1.5 and pAb-nNav1.5 reduced nNav1.5 gene and protein expression in MDA-MB-231 and 4T1 cells

Real-time PCR was used to investigate the effect of the antibodies on nNav1.5 gene expression. Anti-nNav1.5 antibodies were treated to MDA-MB-231 and 4T1 cells for 24 hours, resulting in significant downregulation of the nSCN5A gene, similar to TTX treatment (Figure 2 A i and 2 A ii).

nNav1.5 protein expression was assessed using immunofluorescence assay after 24-hour antibody treatments. The mAb-nNav1.5, pAb-nNav1.5, and TTX treatments resulted in decreased red staining (indicating nNav1.5 protein expression) in the cytoplasm and plasma membrane of MDA-MB-231 and 4T1 cells, as shown by reduced or weak red fluorescence in the cytoplasm and plasma membrane (Figure 2 B, C and D). Untreated cells, on the other hand, exhibited extensive red staining that spanned the majority of the cytoplasm and plasma membrane (Figure 2 B, C and D). Statistical analysis revealed a statistically significant decrease in nNav1.5 protein expression in 4T1 and MDA-MB-231 with mAb-nNav1.5, pAb-nNav1.5 and TTX treated cells compared to untreated cells, $p < 0.05$ and $p < 0.001$, respectively (Figure 2 E and F).

mAb-nNav1.5 and pAb-nNav1.5 significantly suppressed 3D-spheroid invasion of MDA-MB-231 and 4T1 cells

Other than effects on the nNav1.5 gene and protein expression, behavioural effects of the antibodies in cancer cells using 3D-spheroid invasion assay of MDA-MB-231 and 4T1 was conducted. The invasion capacity of the 3D-spheroids MDA-MB-231 and 4T1 culture was significantly reduced by ~30% and ~58%, respectively, after 24 hours treated with mAb-nNav1.5 (1:9), whilst the reduction in pAb-nNav1.5 (3:7) treated groups were 30% and ~50% in MDA-MB-231 and 4T1 cells, respectively (Figure 3 A and B). The reduction can be seen as early

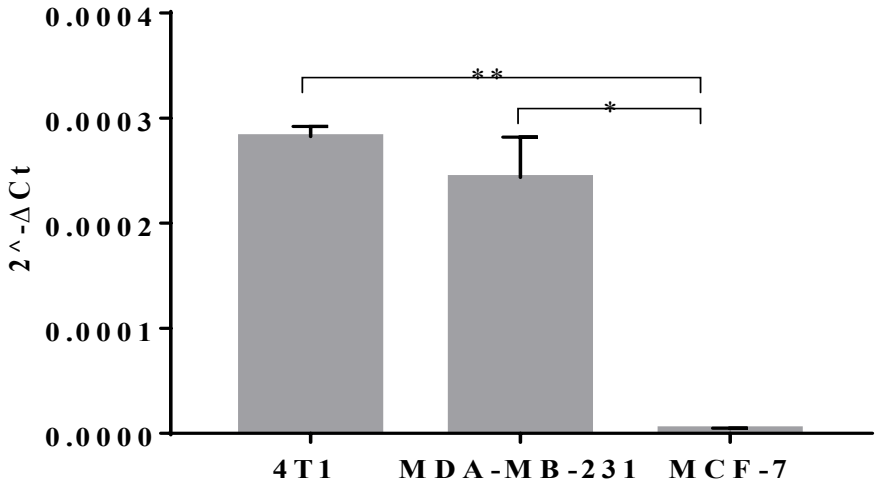

Figure 1. The Bar Graph Depicted the basal mRNA Expression of nNav1.5 in the Invasive Mouse Mammary Cancer Cells, 4T1 and (human breast cancer cells) MDA-MB-231 and weakly invasive human breast cancer cells, MCF-7 cells using Tukey's multiple comparison test where * $p < 0.05$ and ** $p < 0.001$ were considered significant.

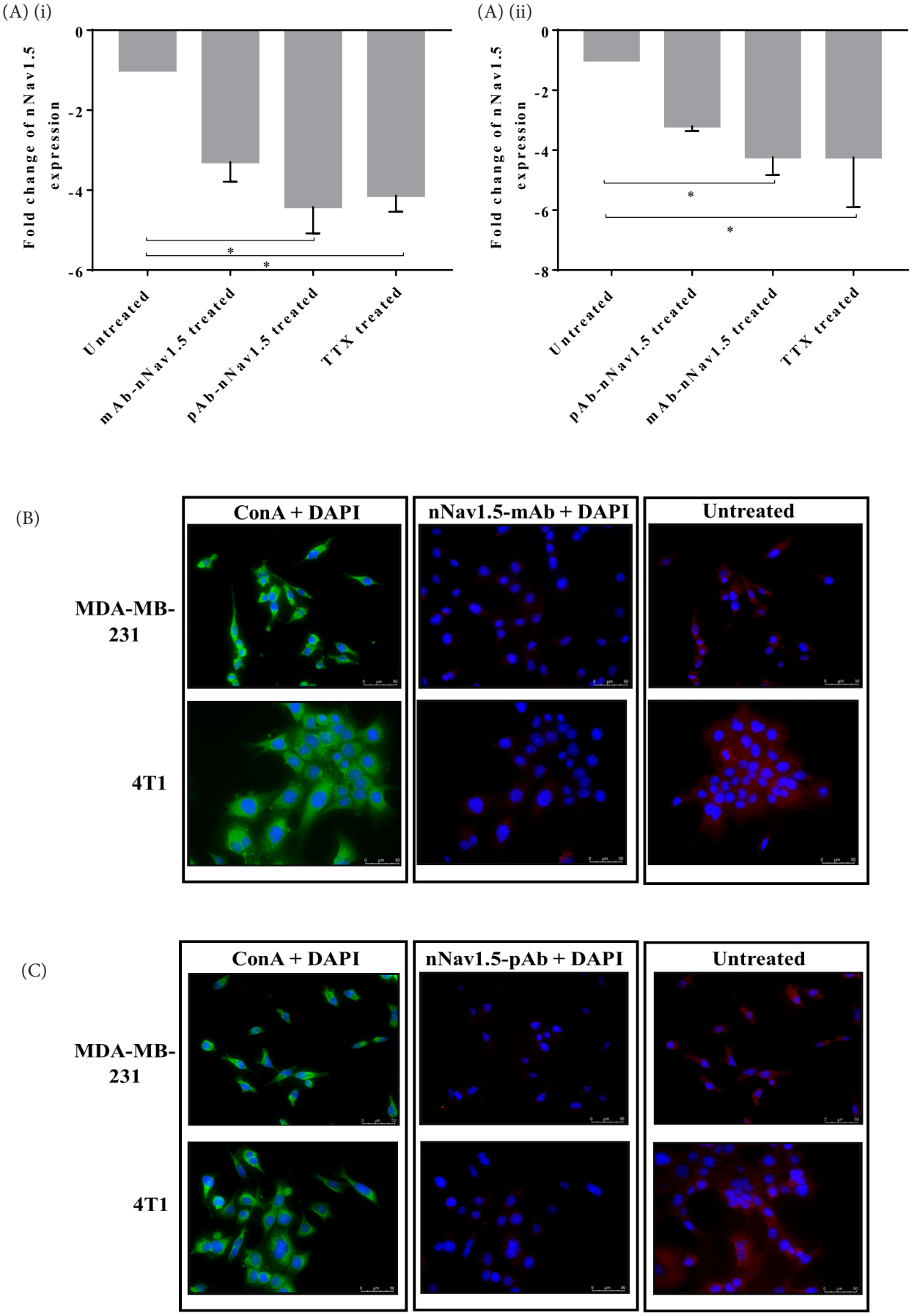

Figure 2. A) The relative mRNA expression was measured using qRT-PCR after 24-hour treatment with pAb-nNav1.5 and mAb-nNav1.5 on (i) MDA-MB-231 and (ii) 4T1 cells, where β-actin and GAPDH were used as housekeeping genes, respectively. Immunofluorescence microscopy images of treated MDA-MB-231 and 4T1 cells with (B) mAb-nNav1.5 (1:10 = 10 µg/ml), (C) pAb-nNav1.5 (1:100 = 59.2 µg/ml)

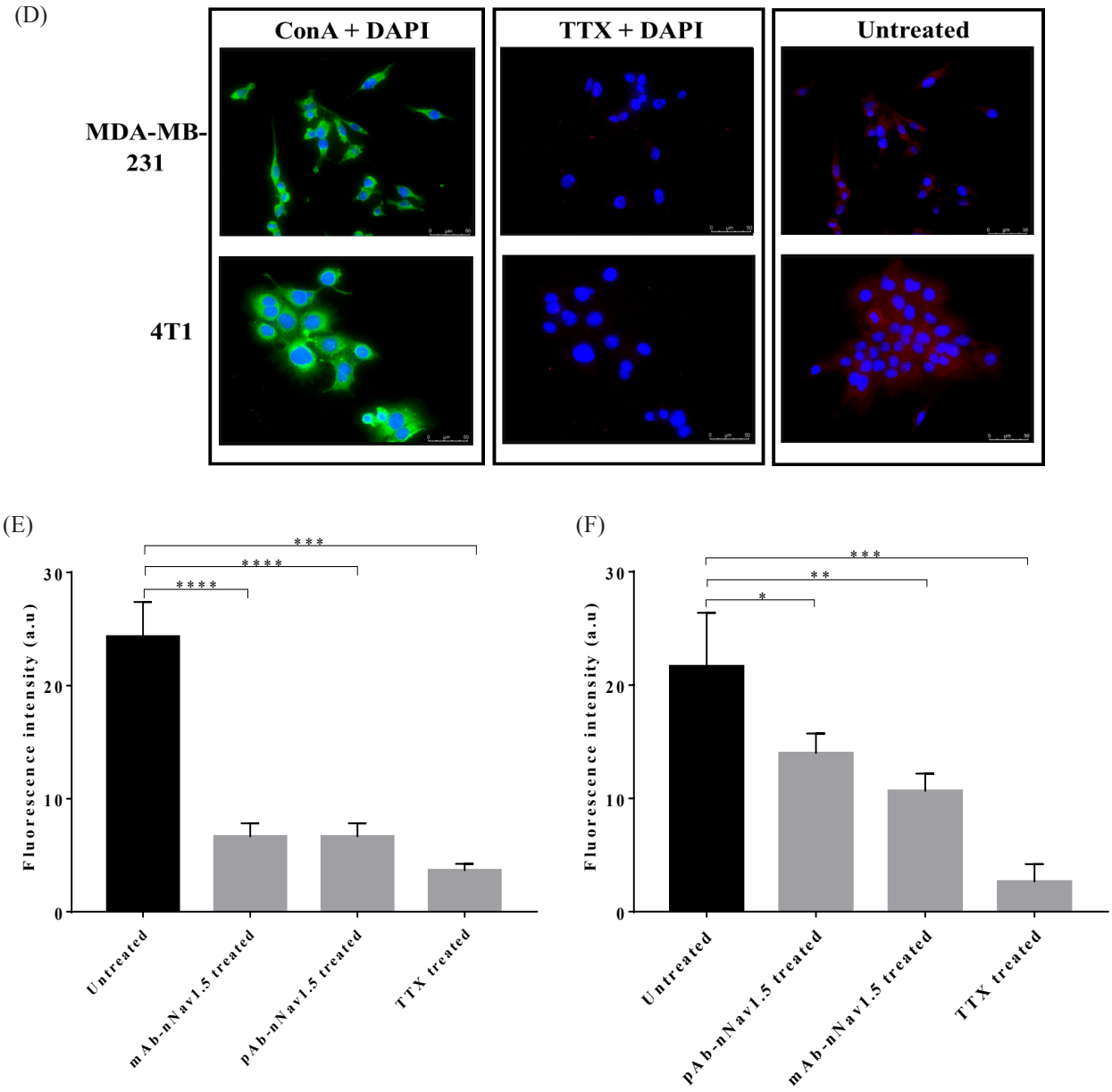

Figure 2. (D) TTX (10 µM) on nNav1.5 protein expression after 24-hour treatment. Blue fluorescence represents nuclear staining by DAPI, and green fluorescence represents the plasma membrane staining by ConA. Red fluorescence represents nNav1.5 staining by pAb-nNav1.5 and mAb-nNav1.5 antibodies; secondary antibody conjugated-Alexa Fluor 555. Images were viewed using Leica Inverted DMi8 fluorescence microscope, Leica Application Software X (LAS X), and captured using DFC 365 FX Camera (Leica Microsystems, Germany) at 40X magnification. Histograms represent the fluorescence intensity of (E) MDA-MB-231 and (F) 4T1 cells in both untreated and treated cells.

as day 1 after treatment in both MDA-MB-231 and 4T1 cells, $p < 0.05$, $p < 0.001$ and $p < 0.0001$ (Figure 3 A ii and Figure 3 B ii). Treatment with 10 µM of TTX reduced the invasion by ~10% and ~50% in MDA-MB-231 and 4T1 cells, respectively (Figure 3 A and B). In addition, mAb-nNav1.5 (1:9) reduced cancer cell invasion by ~60% compared to ~50% and ~30% reductions in TTX and pAb-nNav1.5 (3:7), respectively, for 4T1 cells. In MDA-MB-231 cells, pAb-nNav1.5 (3:7) and mAb-nNav1.5 (1:9) reduced invasion by ~24% and 15%, respectively, followed by a 7% reduction in the TTX-treated group.

Observation of animal's body weight, extracted primary tumours and vital organs in animals treated with mAb-nNav1.5 and pAb-nNav1.5

The body weight was assessed between the last day and day after inoculation of the tumour animal model treated with PBS (control), mAb-nNav1.5, and pAb-nNav1.5. The results revealed an increased mean difference of body weight in the pAb-nNav1.5 and mAb-nNav1.5 treated group compared to PBS treated (Figure 4 A). After euthanisation, the primary tumour was extracted and weighed. The tumour mass of the treated animals was significantly reduced compared to the control group (Figure 4 B). The tumour size after the treatment was also reduced compared to the PBS group (Figure 4 C). Additionally, observation of the extracted organs such as the spleen, lungs, liver, and intestines revealed that in the PBS-treated group, the organs presented with lesions (black circle) and loss of structure in each of the organs

3 (A) (i)

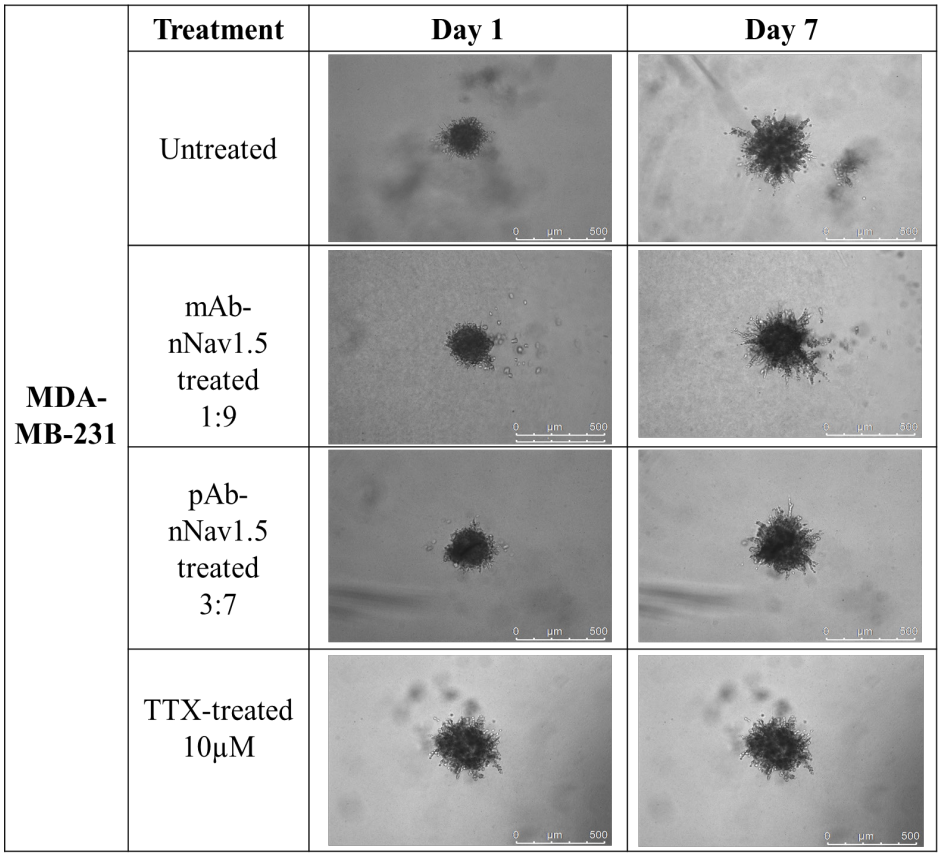

3 (A) (ii)

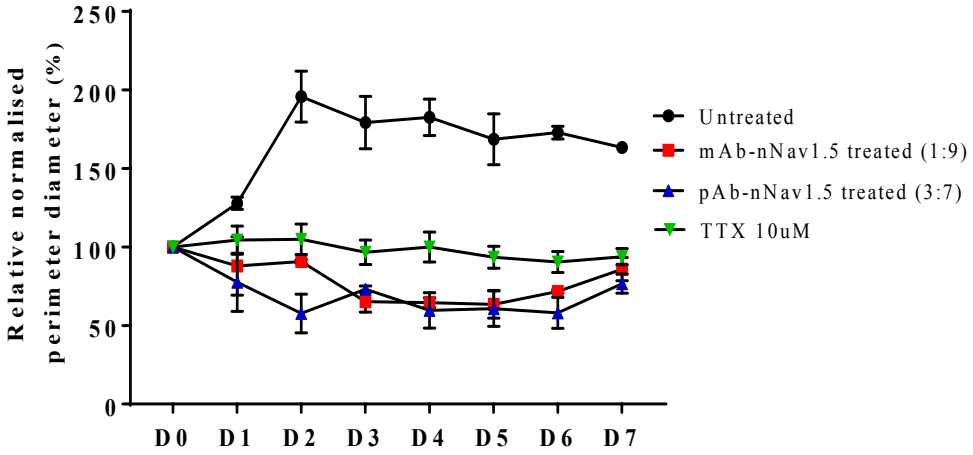

Dunnett's multiple comparisons tests								
Day	0	1	2	3	4	5	6	7
Untreated vs. mAb-nNav1.5 treated (1:9)	ns	***	****	****	****	****	****	****
Untreated vs. pAb-nNav1.5 treated (3:7)	ns	****	****	****	****	****	****	****
Untreated vs. TTX 10uM	ns	*	****	****	****	****	****	****

3 (B) (i)

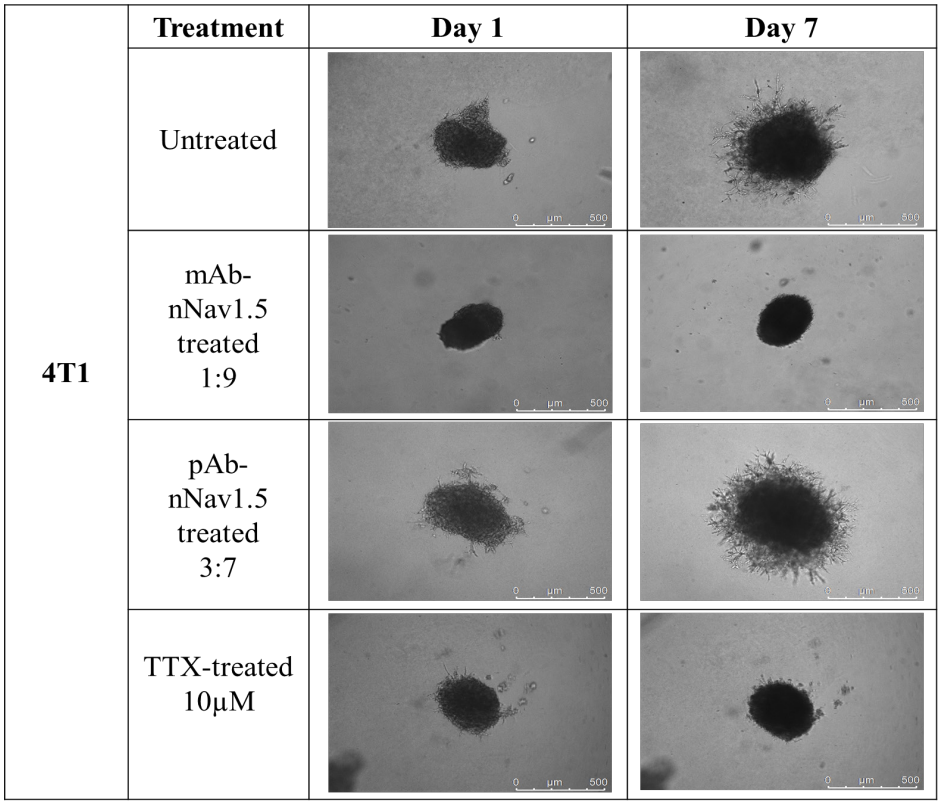

3 (B) (ii)

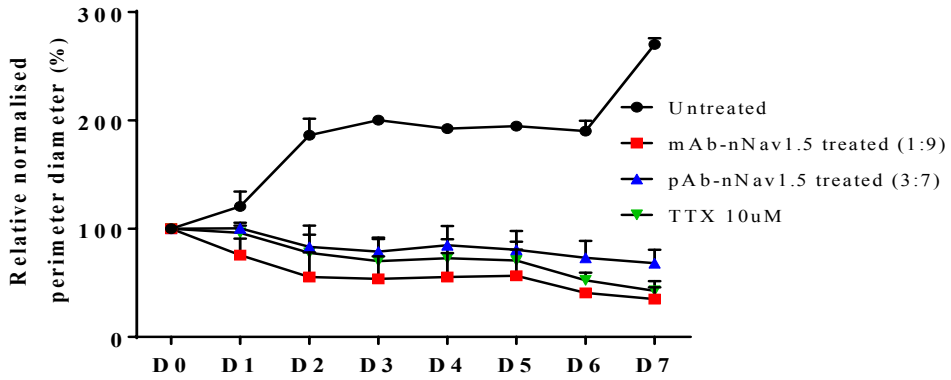

Dunnett's multiple comparisons test								
Day	0	1	2	3	4	5	6	7
Untreated vs. mAb-nNav1.5 treated (1:9)	ns	**	****	****	****	****	****	****
Untreated vs. pAb-nNav1.5 treated (3:7)	ns	ns	****	****	****	****	****	****
Untreated vs. TTX 10uM	ns	ns	****	****	****	****	****	****

Figure 3. Effects of Treatment Agents on the Invasion of Breast Bancer 3D-spheroids. 3D-spheroids of (A) MDA-MB-231 and (B) 4T1 cells lines were treated with mAb-nNav1.5 (1:9 = 54.5 µg/ml), pAb-nNav1.5 (3:7 = 177 µg/ml) and positive control, TTX (10 µM). A i) and B i) 3D-spheroids captured under 10X magnification using Leica inverted fluorescence microscope. The representative 3D-spheroid images were on day 1 (D1) and day 7 (D7). The scale of the image was set at 500 µm. (A ii) and (B ii) Line graph of relative normalised perimeter diameter (%) of treated 3D-spheroids in a duration of seven days treatment and invasion, compared to untreated 3D-spheroids. The invasion of treated 3D-spheroids day 1 (D0) until day 7 (D7) was significantly reduced as compared to untreated 3D-spheroids according to statistical analysis, Dunnett's multiple comparison test, and multiple t-tests. Ns= not-significant, * $p < 0.05$, ** $p < 0.01$, *** $p < 0.001$ and **** $p < 0.0001$.

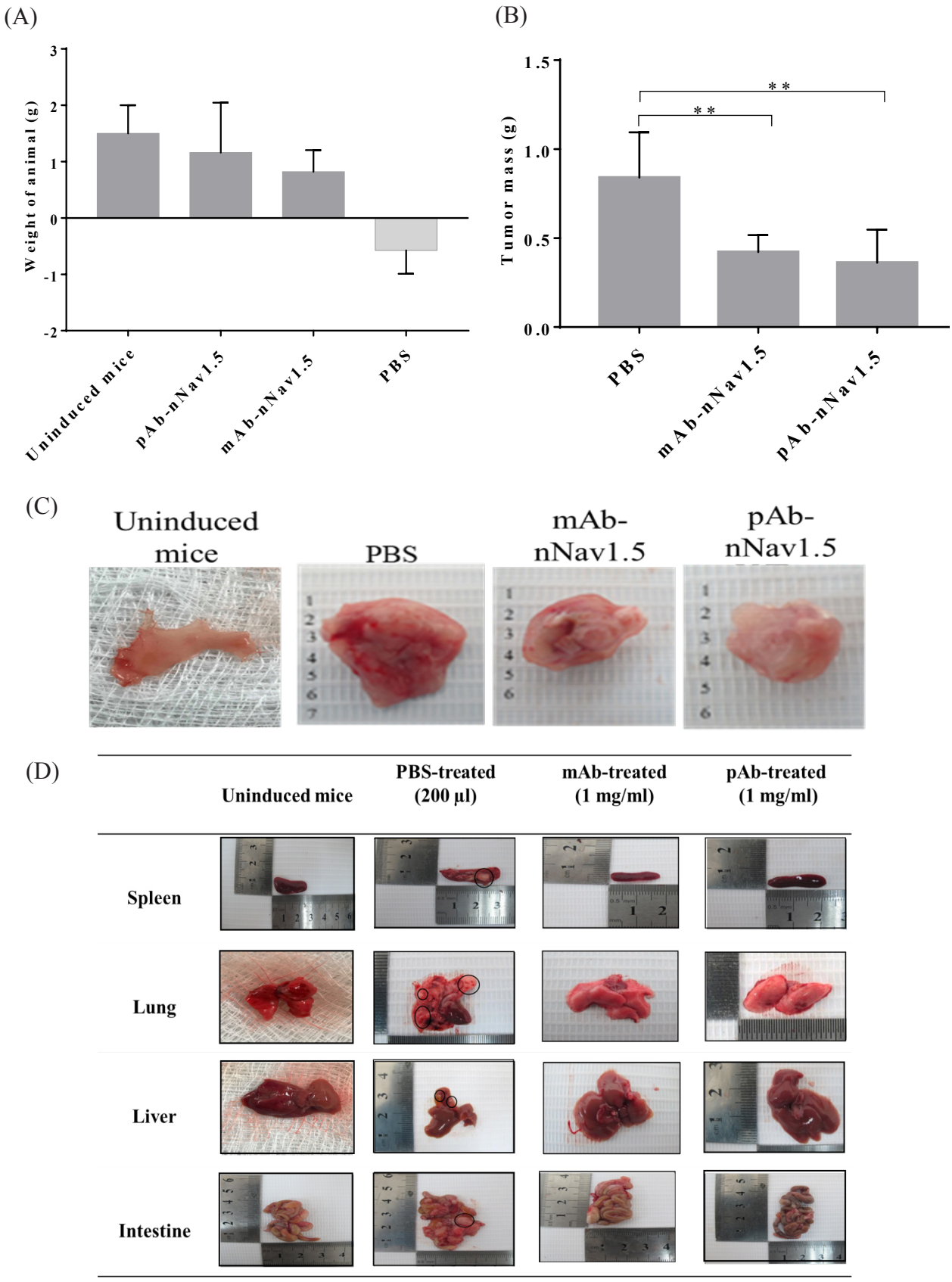

Figure 4. Effects of pAb-nNav1.5 and mAb-nNav1.5 treatments in a syngeneic orthotopic animal model of induced mammary tumour BALB/c female mice with 4T1 cells. A) Bar graph represents the mean difference of body weight between the last day of the animal before euthanisation and the day after inoculation of the tumour animal model treated with mAb-nNav1.5 (1 mg/ml) and pAb-nNav1.5 (1 mg/ml) compared to tumour animal model treated with PBS. B) Bar graph represents the mean of tumour mass reduced in the treatment group compared to the control group. C) Representative images of extracted tumours from animals in each group. The extracted tumours reduced in size in the treated group compared to the control group. D) Representative images of extracted organs where black circle indicates macro-metastatic lesions. Statistical analysis was performed using One-Way ANOVA, ** $p < 0.01$ was considered significant.

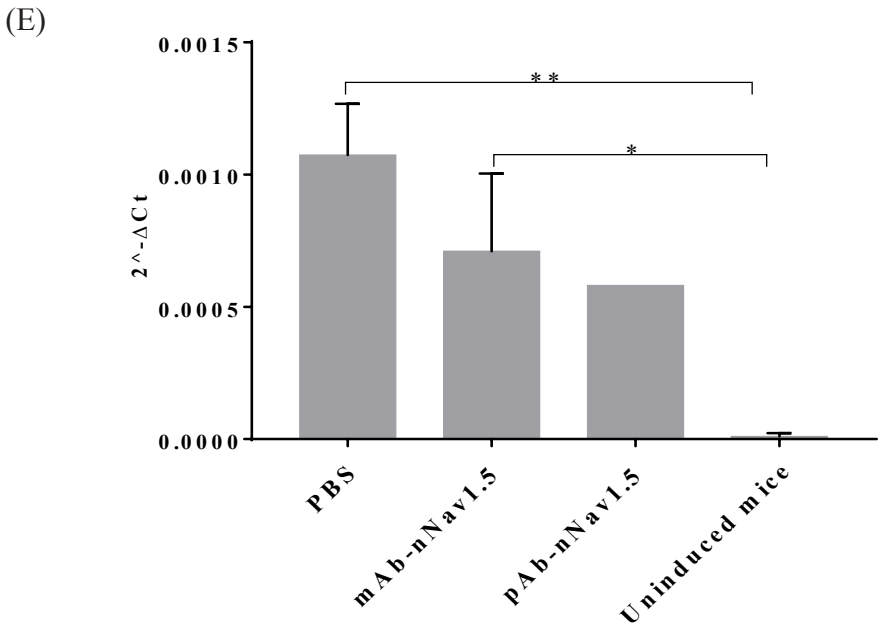

Figure 4. E) The bar graph depicted the mRNA expression of nNav1.5 in the primary tumours of each experimental group's animals using Tukey's multiple comparison test.

(Figure 4 D). On the contrary, the pAb-nNav1.5 and mAb-nNav1.5 treated groups presented with no occurrence of lesions with intact organ structures (Figure 4 D).

mAb-nNav1.5 and pAb-nNav1.5 reduced nNav1.5 gene expression in tumor tissues of treated animal

Aside from observing tumour size and mass in all experimental groups, the extracted primary tumours were evaluated and compared for nSCN5A expression using real-time PCR between the PBS-treated group to the pAb-nNav1.5 and mAb-nNav1.5 treated groups. Results revealed that nSCN5A expression was decreased in the antibodies-treated groups compared to the PBS group. The expression of nSCN5A in the mAb-nNav1.5 treated group compared to the uninduced mice was considered significant following One-Way ANOVA statistical analysis (Figure 4 E).

Discussion

The first proof-of-concept that supports the therapeutic value of nNav1.5 in targeting breast cancer aggressiveness was raised when treatment with TTX inhibits various in vitro activities associated with metastatic behaviours such as galvanotaxis, endocytic membrane activity, migration and invasion of breast cancer cells, MDA-MB-231 cells (Fraser et al., 2005) - MDA-MB-231 is famously known for its aggressive characteristics also the original cell type where nNav1.5 was first discovered (Fraser et al., 2005). Subsequent data on the effect of other VGSCs modulator drugs, e.g., propranolol and phenytoin (Yang et al., 2012; Nelson, Yang Dowle et al., 2015; Lee et al., 2019), as well as siRNA/shRNA-nNav1.5 on the cells, revealed similar results (Gillet et al., 2009; Guzel et al., 2019). Subsequent works on developing an antibody against nNav1.5 successfully produced a rabbit-polyclonal antibody, NESOpAb (Chioni et al., 2005), which it also has been demonstrated to effectively inhibit migration and invasion of MDA-MB-231 cells comparable to TTX (Fraser et al., 2014). Although few of these drugs, i.e., phenytoin and ranolazine, including TTX, have been demonstrated to inhibit metastasis in vivo (Nelson, Yang, Dowle et al., 2015; Nelson, Yang, Millican-Slater et al., 2015), however, NESOpAb has never been tested in animal model. With the motivation to investigate the effect of anti-nNav1.5 antibodies in the animal model, this study was designed where mouse monoclonal and polyclonal antibody against nNav1.5 was obtained. The antibodies were raised in mice to match the animal model used in this study. Moreover, higher expression of nSCN5A expression in 4T1 cells, a mouse aggressive mammary tumor cells, supported the strategy to use this cell to inoculate into the animal model. Interestingly, the effectiveness of mAb-nNav1.5 and pAb-nNav1.5 in inhibiting invasion was not only observed in 3D-spheroid culture of 4T1 cells but also in MDA-MB-231 cells. In fact, the effect of these antibodies in suppressing invasion in both cell types was greater than TTX. In the subsequent experiments, treatment with these antibodies also effectively downregulate nSCN5A/nNav1.5 expression in MDA-MB-231 and 4T1 cells as demonstrated by reduced red staining in immunofluorescence staining and decreased fold level in real-time PCR analysis.

In the in vivo experiment, our findings revealed that the 4T1-induced mammary tumour mouse model treated with mAb-nNav1.5 and pAb-nNav1.5 retained healthy body weight and appeared to have a significantly smaller tumour mass (size and weight) than the PBS control group. Importantly, treatment with the antibodies revealed no lesions in the organs such as the lung, liver, spleen, and intestines compared to the PBS control group, where inflamed lesions were observed. These findings are essential in demonstrating that the new anti-nNav1.5 antibodies can achieve similar efficacy in preventing

metastasis in mammary tumour animal models comparable to in vitro. Accordingly, inhibition of metastasis by mAb-nNav1.5 and pAb-nNav1.5 corresponded with downregulation of nSCN5A expression in the tumour tissues. Previously, Gao et al. (2019) showed that an antibody targeting adult Nav1.5, E3, exerts an inhibitory effect on tumour growth and invasion in ovarian cancer animal model (Gao et al., 2019) – in ovarian cancer, Nav1.5 is one of the major VGSCs subtype expressed and associated with aggressiveness (Altamura et al., 2021).

Previous studies on the regulation of VGSCs in breast cancer discovered that their expression is regulated via activity-dependent positive auto-regulation (Chioni et al., 2010). Blocking of VGSCs channels activity (measured using electrophysiology) using TTX, small molecule inhibitors, siRNA/shRNA, and NESOpAb (Brackenbury and Djamgoz, 2006; Brackenbury et al., 2007) disrupts this auto-regulation loop, thus inhibiting VGSC's expression and is adequate to suppress invasion or metastatic behaviours (Brackenbury and Djamgoz, 2006; Brackenbury et al., 2007). In agreement to this, in the present study, mAb-nNav1.5 and pAb-nNav1.5 significantly downregulate nNav1.5 protein and gene expression, indicating that disturbance of the VGSCs auto-regulation loop have led to the inhibition of invasion in vitro and metastasis in vivo.

In summary, detectable nNav1.5 expression is associated with the population of patients with poor prognosis, i.e., advanced stage positive for lymph node metastasis and recurrence (Brackenbury, 2012; Dutta et al., 2018) and triple-negative breast cancer (TNBC) subtype (Lee et al., 2019). This study's findings add to the early effort using NESOpAb, utilising antibodies in targeting nNav1.5 for combating breast cancer metastasis – comparable to NESOpAb mAb-nNav1.5 and pAb-nNav1.5 produced significant therapeutic effect in suppressing nNav1.5-dependent breast cancer invasiveness in vitro and metastasis in vivo. The use of these specific antibodies in targeting nNav1.5 could be an alternative to TTX or small molecule drugs where toxicity concerns have been raised.

Author Contribution Statement

Conception: N.F.M., N.S.Y., A.A.D., and M.E.S; Interpretation or analysis of data: N.A.S., A.H.M, I. I and M.M.A; Preparation of the manuscript: N.F.M, N.A.S; Revision for important intellectual content: N.F.M., N.S.Y., A.A.D., and M.E.S; Supervision: N.F.M.

Acknowledgments

This research was funded by the Ministry of Energy, Science, Technology, Environment and Climate Change (MESTECC), Malaysia, under the Science Fund (Grant no: 06-01-05-SF0844). We also appreciate the support of the Malaysian Ministry of Education through the Higher Institution Centre of Excellence (HICoE) Program (No. 311/CIPPM/4401005) and Majlis Amanah Rakyat (MARA) for the student's financial assistance.

Statement conflict of Interest

None

References

Altamura C, Greco MR, Carratù MR, et al (2021). Emerging roles for ion channels in ovarian cancer: Pathomechanisms and pharmacological treatment. *Cancers*, **13**, 1–28.

Bennett ES, Smith BA, Harper JM (2004). Voltage-gated Na+ channels confer invasive properties on human prostate cancer cells. *Eur J Physiol*, **447**, 908–14.

Brackenbury WJ (2012). Voltage-gated sodium channels and metastatic disease. *Channels*, **6**, 352–61.

Brackenbury WJ, Chioni AM, Diss JKJ, Djamgoz MBA (2007). The neonatal splice variant of Nav1.5 potentiates in vitro invasive behaviour of MDA-MB-231 human breast cancer cells. *Breast Cancer Res Treat*, **101**, 149–60.

Brackenbury WJ, Djamgoz MBA (2006). Activity-dependent regulation of voltage-gated Na+ channel expression in Mat-LyLu rat prostate cancer cell line. *J Physiol*, **573**, 343–56.

Brisson L, Gillet L, Calaghan S, et al (2011). Nav1.5 enhances breast cancer cell invasiveness by increasing NHE1-dependent H efflux in caveolae. *Oncogene*, **30**, 2070–6.

Chioni AM, Fraser SP, Pani F, et al (2005). A novel polyclonal antibody specific for the Nav1.5 voltage-gated Na+ channel "neonatal" splice form. *J Neuroscience Methods*, **147**, 88–98.

Chioni AM, Shao D, Grose R, Djamgoz MBA (2010). Protein kinase A and regulation of neonatal Nav1.5 expression in human breast cancer cells: Activity-dependent positive feedback and cellular migration. Int J Biochem Cell Biol, **42**, 346–58.

Diss JKJ, Fraser SP, Djamgoz MB a (2004). Voltage-gated Na+ channels: multiplicity of expression, plasticity, functional implications and pathophysiological aspects. *Eur Biophys J*, **33**, 180–93.

Driffort V, Gillet L, Bon E, et al (2014). Ranolazine inhibits NaV1.5-mediated breast cancer cell invasiveness and lung colonization. *Mol Cancer*, **13**, 1–6.

Dutta S, Charcas OL, Tanner S, et al (2018). Discovery and evaluation of nNav 1.5 sodium channel blockers with potent cell invasion inhibitory activity in breast cancer cells. *Bioorganic Med Chem Lett*, **26**, 2428–36.

Faustino-Rocha A, Oliveira PA, Pinho-Oliveira J, et al (2013) Estimation of rat mammary tumor volume using caliper and ultrasonography measurements. *Lab Animal*, **42**, 217–24.

Fraser SP, Salvador V, Manning EA, et al (2003). Contribution of functional voltage-gated Na+ channel expression to cell behaviors involved in the metastatic cascade in rat prostate cancer: I. Lateral motility. *J Cell Physiol*, **195**, 479–87.

Fraser SP, Diss JKJ, Chioni AM, et al (2005). Voltage-gated sodium channel expression and potentiation of human breast cancer metastasis. *Clin Cancer Res*, **11**, 5381–9.

Fraser SP, Ozerlat-Gunduz I, Brackenbury WJ, et al (2014) Regulation of voltage-gated sodium channel expression in cancer: Hormones, growth factors and auto-regulation. *Philos Trans R Soc Lond B Biol Sci*, **369**, 1–12.

Gao R, Cao T, Chen H, et al (2019). Nav1.5-E3 antibody inhibits cancer progression. *Transl Cancer Res*, **8**, 44–50.

Hanahan D, Weinberg RA (2011). Hallmarks of cancer: The next generation. *Cell*, **144**, 646–74.

House CD, Vaske CJ, Schwartz AM, et al (2010). Voltage-gated Na+ channel SCN5A is a key regulator of a gene transcriptional network that controls colon cancer invasion. *Cancer Res*, **70**, 6957–67.

Lee A, Fraser SP, Djamgoz MBA (2019). Propranolol inhibits neonatal Nav1.5 activity and invasiveness of MDA-MB-231 breast cancer cells: Effects of combination with ranolazine.

J Cell Physiol, **234**, 23066–81.
Livak KJ, Schmittgen TD (2001). Analysis of relative gene expression data using real-time quantitative PCR and the $2^{-\Delta\Delta CT}$ method. *Methods*, **25**, 402–8.
Lu RM, Hwang YC, Liu IJ, et al (2020). Development of therapeutic antibodies for the treatment of diseases. *J Biomed Sci*, **27**, 1–30.
Nelson M, Yang M, Dowle AA, et al (2015). The sodium channel-blocking antiepileptic drug phenytoin inhibits breast tumour growth and metastasis. *Mol Cancer*, **14**, 1–7.
Nelson M, Yang M, Millican-Slater R, Brackenbury WJ (2015). Nav1.5 regulates breast tumor growth and metastatic dissemination in vivo. *Oncotarget*, **6**, 32914–29.
Onkal R, Djamgoz MBA (2009). Molecular pharmacology of voltage-gated sodium channel expression in metastatic disease: Clinical potential of neonatal Nav1.5 in breast cancer. *Eur J Pharmacol*, **625**, 206–19.
Roger S, Rollin J, Barascu A, et al (2007). Voltage-gated sodium channels potentiate the invasive capacities of human non-small-cell lung cancer cell lines. *Int J Biochem Cell Biol*, **39**, 774–86.
Rosas-Arellano A, Villalobos-González JB, Palma-Tirado L, et al (2016). A simple solution for antibody signal enhancement in immunofluorescence and triple immunogold assays. *Histochem Cell Biol*, **146**, 421–30.
Russo J (2016). The pathobiology of breast cancer, The Pathobiology of Breast Cancer. Switzerland: Springer International Publishing.
Wang J, Ou SW, Wang YJ (2017). Distribution and function of voltage-gated sodium channels in the nervous system. *Channels*, **11**, 534–54.
Xia J, Huang N, Huang H, et al (2016). Voltage-gated sodium channel Nav1.7 promotes gastric cancer progression through MACC1-mediated upregulation of NHE1. *Int J Cancer*, **139**, 2553–69.
Yamaci RF, Fraser SP, Battaloglu E, et al (2017). Neonatal Nav1.5 protein expression in normal adult human tissues and breast cancer. *Pathol Res Pract*, **213**, 900–7.
Yang M, Kozminski DJ, Wold LA, et al (2012). Therapeutic potential for phenytoin: Targeting Nav1.5 sodium channels to reduce migration and invasion in metastatic breast cancer. *Breast Cancer Res Treat*, **134**, 603–15.